

**Zeitschrift:** Schweizerische mineralogische und petrographische Mitteilungen = Bulletin suisse de minéralogie et pétrographie  
**Band:** 75 (1995)  
**Heft:** 3  
  
**Artikel:** Titanite-rich carbonates from the Therapio area in Thrace, Northern Greece : constraints of the mineral assemblage formation  
**Autor:** Kassoli-Fournaraki, A. / Michailidis, K. / Zannas, I.  
**DOI:** <https://doi.org/10.5169/seals-57163>

### **Nutzungsbedingungen**

Die ETH-Bibliothek ist die Anbieterin der digitalisierten Zeitschriften auf E-Periodica. Sie besitzt keine Urheberrechte an den Zeitschriften und ist nicht verantwortlich für deren Inhalte. Die Rechte liegen in der Regel bei den Herausgebern beziehungsweise den externen Rechteinhabern. Das Veröffentlichen von Bildern in Print- und Online-Publikationen sowie auf Social Media-Kanälen oder Webseiten ist nur mit vorheriger Genehmigung der Rechteinhaber erlaubt. [Mehr erfahren](#)

### **Conditions d'utilisation**

L'ETH Library est le fournisseur des revues numérisées. Elle ne détient aucun droit d'auteur sur les revues et n'est pas responsable de leur contenu. En règle générale, les droits sont détenus par les éditeurs ou les détenteurs de droits externes. La reproduction d'images dans des publications imprimées ou en ligne ainsi que sur des canaux de médias sociaux ou des sites web n'est autorisée qu'avec l'accord préalable des détenteurs des droits. [En savoir plus](#)

### **Terms of use**

The ETH Library is the provider of the digitised journals. It does not own any copyrights to the journals and is not responsible for their content. The rights usually lie with the publishers or the external rights holders. Publishing images in print and online publications, as well as on social media channels or websites, is only permitted with the prior consent of the rights holders. [Find out more](#)

**Download PDF:** 13.08.2025

**ETH-Bibliothek Zürich, E-Periodica, <https://www.e-periodica.ch>**

## **Titanite-rich carbonates from the Therapio area in Thrace, Northern Greece: constraints of the mineral assemblage formation**

by A. Kassoli-Fournaraki<sup>1</sup>, K. Michailidis<sup>1</sup>, I. Zannas<sup>2</sup> and S. Zachos<sup>3</sup>

### **Abstract**

The present study examines the mineral composition and paragenesis of titanite-rich impure marbles and calc-silicate rocks, occurring as layers in pure marbles and amphibolites/gneisses in the Therapio area of Thrace, Northern Greece. These lithologies are crosscut by a network of pegmatite veins. The main mineral constituents are calcite, titanite, amphibole, clinopyroxene, plagioclase, zoisite, clinozoisite and quartz with minor chlorite and mica. Chemistry and mineralogic composition of the impure marble and calc-silicate layers are attributed to inhomogeneities of the sedimentary protoliths enhanced by metasomatic processes related to an amphibolite-facies metamorphism. Additional compositional variations in the minerals were caused by the pegmatite vein formation. Temperatures of 540–660 °C and pressures not exceeding 7 kbar are inferred for the studied carbonate rocks, according to the observed mineral equilibria and phase reaction diagrams. The minerals formed, imply a high activity of H<sub>2</sub>O relative to CO<sub>2</sub> for the metasomatic fluid.

**Keywords:** titanite, calc-silicates, impure marble, metamorphism, metasomatism, Therapio, Rhodope massif, Greece.

### **Introduction**

Titanite is a common accessory mineral found in a large variety of rock types (DEER et al., 1982). Studies of titanite-bearing metamorphic assemblages (e.g., BUDDINGTON et al., 1963; MAKANJOULA and HOWIE, 1972; HARLEY and BUICK, 1992) and experimental determination of titanite stability relations (e.g., COOMBS et al., 1976; HUNT and KERRICK, 1977) suggest that titanite is a useful mineral phase for constraining P-T-X<sub>CO<sub>2</sub></sub> conditions of metamorphism. In addition, its chemistry is controlled by many variables such as bulk composition, fluid phase, and grade of metamorphism (e.g., FRANZ and SPEAR, 1985; GILBERT et al., 1990; GRAPES and WATANABE, 1992).

In the present study, the composition of titanite and its paragenesis in the impure marbles and calc-silicate rocks of the Therapio area are

examined. The purpose of this study is to focus on the metamorphism of the titanite-bearing carbonate rocks and to attempt an interpretation of the mineral formation by clarifying the relationships between reaction textures and mineral equilibria.

### **Location and petrography**

The investigated area is situated 2 km northwest of the village Therapio, in Evros County of Northern Greece (Fig. 1). Geotectonically, it belongs to the "Upper Tectonic Unit" (according to PAPANIKOLAOU and PANAGOPOULOS, 1981) or to the "Low Marble-amphibolite Series" (according to DIMADIS and ZACHOS, 1989) of the Rhodope massif. The Rhodope massif of Northern Greece mainly consists of metamorphic rocks, including

<sup>1</sup> Department of Mineralogy, Petrology, Economic Geology, School of Geology, University of Thessaloniki, Thessaloniki 54006, Greece. e-mail: kassoli@olymp.ccf.auth.gr

<sup>2</sup> I.G.M.E. Thessaloniki, Frankon 1, Thessaloniki 54626, Greece.

<sup>3</sup> I.G.M.E. Xanthi, Brokoumi 30, Xanthi 67100, Greece.

marbles, schists, augen gneisses, pelitic gneisses, and amphibolites.

In the area to the northwest of Therapio, the marble includes layers of calc-silicate rocks, schists, gneisses and amphibolites. A network of veins of pegmatitic composition, ranging in thickness from some cm up to 1.5 m, crosscut the above lithologies. The rocks of the study area have been subdivided as follows:

1. Marbles
2. Impure marbles
3. Calc-silicate rocks
4. Amphibole gneisses and amphibolites
5. Pegmatite veins

With the exception of the pegmatitic veins, the above rocks are mainly interlayered. The calc-silicates form thin layers or boudins in the marbles.

Minerals present were determined optically in thin sections, and the assemblages of representative samples are given in table 1. As can be seen,

the marbles are mostly monomineralic, with calcite as major phase, and with minor muscovite. Traces of quartz, zoisite and plagioclase were noticed locally, particularly in sites adjacent to calc-silicate layers. The mineral assemblage of the calc-silicate layers consists of titanite, calcite, zoisite/clinozoisite, clinopyroxene, plagioclase (oligoclase), amphibole and quartz; the same minerals plus chlorite and mica (biotite, muscovite) are also observed in the impure marbles. The texture in all the above rock types is granoblastic.

Calcite occurs as coarse to medium sized crystals, is multitwinned and often deformed. Recrystallization of calcite grains is frequently observed mainly at the rims of the coarse grains.

Amphibole occurs both as magnesiohornblende and as actinolitic hornblende. Magnesiohornblende was initially formed and exists mainly as relics within clinopyroxene (Fig. 2). Actin-

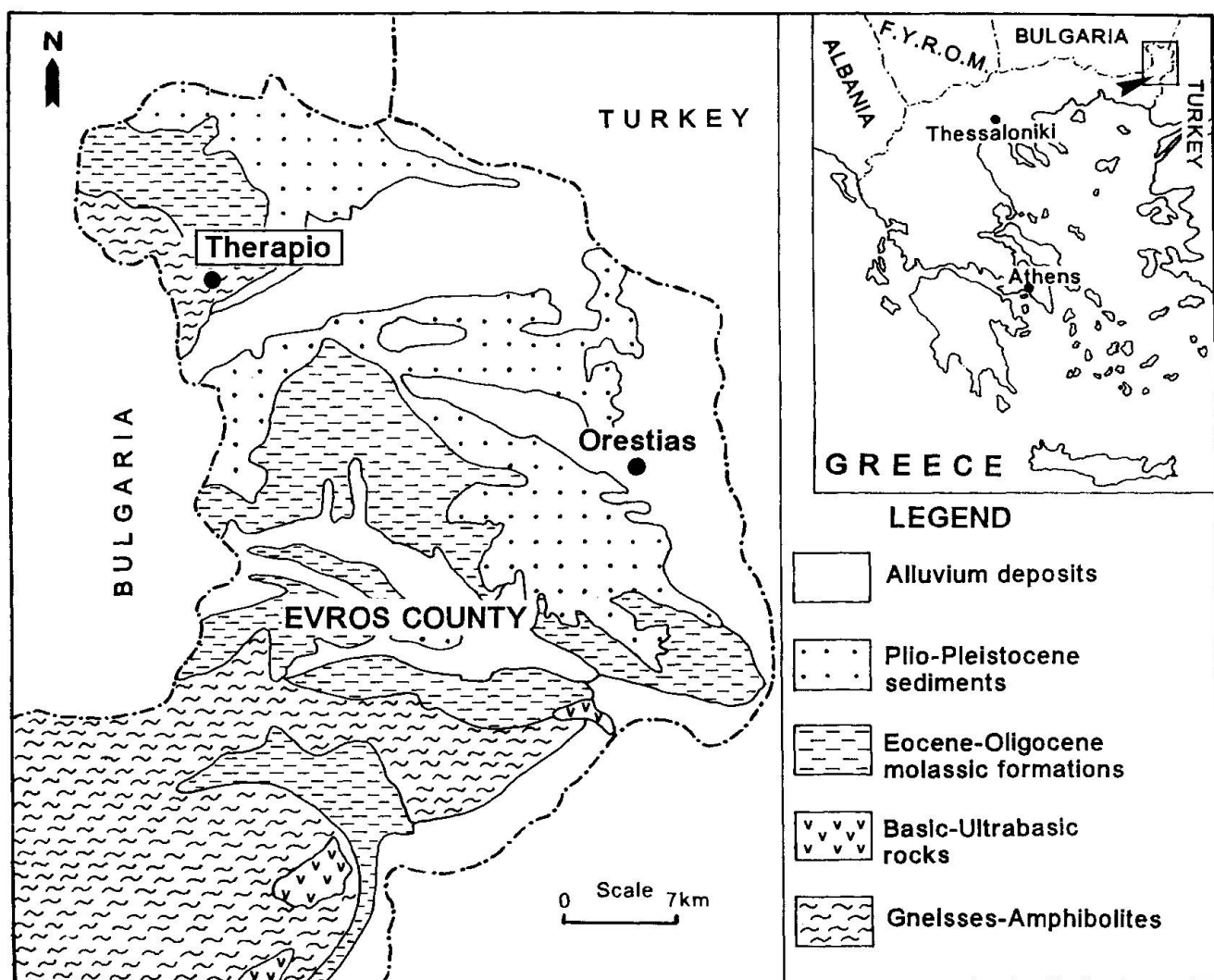


Fig. 1 Simplified geologic sketch map of Eastern Rhodope massif, Northern Greece, and geographic position of the Therapio area.

Tab. 1 Mineralogy of the Therapio main lithologies.

Sample	Rock type	Minerals present										
		Cc	Ti	Zo/cZo	Pl	Py	Am	Qz	Bi	Mu	Chl	K-F
Th-1	Marble	+								±		
Th-2	Marble	+										
Th-3	Impure marble	+	+	+	+			+	+	+	+	
Th-4	Impure marble	+	+	+		+	+	+	+	+		
Th-5	Calc-silicate		+	+		+		+				
Th-6	Pegmatite				+			+	+	+		+
Th-7	Amphibole gneiss		+	+	+		+	+	+			
Th-8	Impure marble	+	+	+				+			+	
Th-9a	Calc-silicate		+	+		+		+			+	
Th-9b	Calc-silicate	+	+	+	+	+		+			+	
Th-9c	Calc-silicate	+	+	+	+	+		+	+			
Th-9d	Calc-silicate	+	+	+	+	+	+		+			
Th-9e	Calc-silicate	+	+	+	+	+	+					
Th-10	Impure marble	+		+	+		+				+	
Th-12	Calc-silicate	+	+	+				+		+		
Th-13	Marble	+								±		

Cc = calcite, Ti = titanite, Zo = zoisite, cZo = clinozoisite, Pl = plagioclase, Py = pyroxene, Am = amphibole, Qz = quartz, Bi = biotite, Mu = muscovite, Chl = chlorite, K-F = K-feldspar

olitic hornblende results from the breakdown of either clinopyroxene or magnesiohornblende, and thus is clearly younger than magnesiohornblende. Quartz is released during these replacements, and calcite plus titanite accompany the reactions. Quartz and calcite are commonly found in contact, without sign of reaction to produce wollastonite. Intergrowths of actinolitic hornblende and clinopyroxene are abundant and document the replacement. Complex poikilitic structures of clinopyroxene, magnesiohornblende, actinolitic hornblende and quartz are frequently observed (Fig. 2). "Myrmekitic" quartz inclusions in amphibole are also noticed. In many cases, plagioclase, formed at the expense of amphibole, is observed as inclusions in magnesiohornblende. More rarely, thin laths of muscovite were observed to be enclosed by amphibole. Zoisite frequently forms at the expense of magnesiohornblende. This intergrowth is always accompanied by quartz and sometimes by calcite.

Titanite occurs mostly as disseminated euhedral to subhedral crystals (Fig. 3), is sometimes twinned, and ranges in size from 1 mm up to more than 2 cm. Occasionally, it contains small inclusions of quartz, calcite and/or plagioclase. It is also found in intergrowths with magnesiohornblende.

Zoisite/clinozoisite occur as large subhedral to anhedral crystals which frequently display strong optical zonation (Fig. 4). Backscattered electron images revealed that the mineral is ei-

ther concentrically zoned or displays a patchy zonation. The cores are mostly zoisite, sometimes forming intergrowths with muscovite. The rims consist of younger clinozoisite, which replaces zoisite with plagioclase accompanying the reaction. Zoisite is also found as a reaction product between plagioclase and calcite. Characteristic intergrowths of zoisite or clinozoisite with plagioclase, titanite, calcite or quartz, are frequently observed. Sometimes, when clinozoisite crystals occur between calcite grains, fine laths of muscovite are observed as coronae around clinozoisite.

Plagioclase occurs either as individual anhedral to subhedral twinned crystals or as inclusions in clinopyroxene, titanite, amphibole, and clinozoisite.

## Chemistry

### ANALYTICAL TECHNIQUES

Microprobe analyses were carried out on a LINK AN 10000 EDS microanalyzer. The following operating conditions were chosen: 15 kV accelerating voltage, beam current 3 nA, surface electron beam of 1 µm diameter, and counting time 100 seconds. Corrections were made using the ZAF-4/FLS software provided by LINK. Natural minerals or synthetic equivalents and pure metals were used as probe standards.

Bulk-rock chemical analyses were obtained by atomic absorption spectroscopy (Perkin-



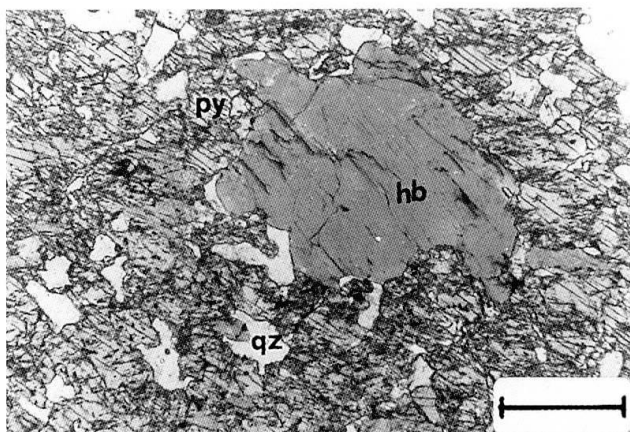


Fig. 2 Relic magnesiohornblende (hb) within poicilitic assemblage of pyroxene (py) + quartz (qz). Scale bar = 0.5 mm.

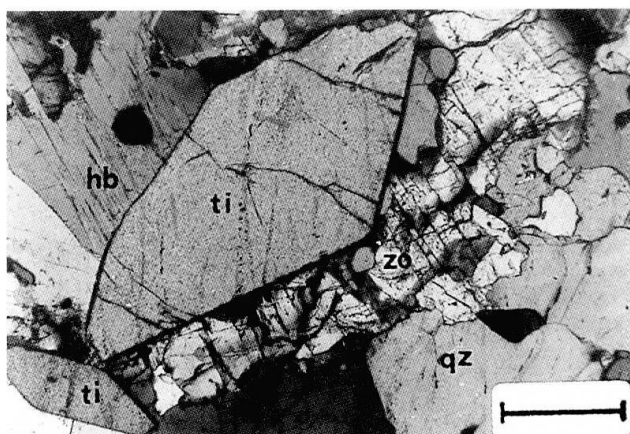


Fig. 3 Titanite (ti) euhedral crystals associated with zoisite (zo), magnesiohornblende (hb) and quartz (qz). Scale bar = 0.5 mm.

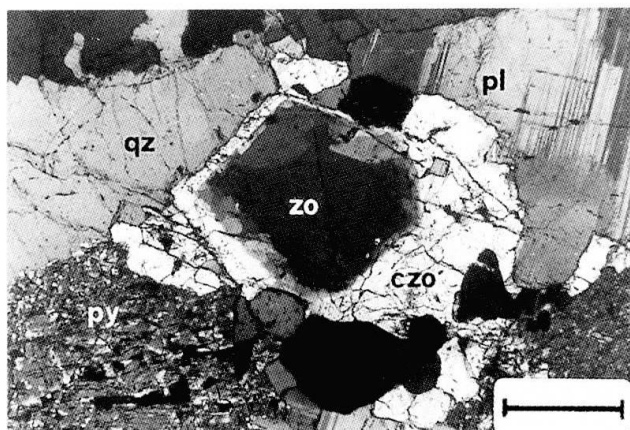


Fig. 4 Strongly zoned zoisite/clinozoisite (zo/czo) grain, associated with quartz (qz), plagioclase (pl) and pyroxene (py). Scale bar = 0.5 mm.

Elmer PE-603) performed on solutions obtained by acid digestion of whole-rock powders.

Calculation and display of P-T-X phase diagrams was performed using the GEOCALC software (BERMAN et al., 1987).

#### MINERAL CHEMISTRY

Representative analyses of the main mineral phases occurring in the carbonates, are given in tables 2 and 3. Total iron is expressed as  $\text{Fe}_2\text{O}_3$  in the minerals titanite and zoisite/clinozoisite, and as FeO in the other phases.

*Titanite.* Two normalization procedures were tried for calculating the structural formula: one on the basis of 5 oxygen atoms and the second on the basis of  $\Sigma$  cations = 3.000. No considerable difference resulted, and thus the normalization on the basis of 5 (O) is presented in table 2. Fluorine, though possibly present (e.g., FRANZ and SPEAR, 1985; GIERÉ, 1992), could not be analyzed by EDS.

The major oxide CaO shows a variation between 27.51 and 29.58 but, except for a few analyses, most values are close to the ideal value (28.60 wt%) for pure titanite.  $\text{SiO}_2$  shows a slightly larger variation (28.43 and 31.14) than CaO, especially towards values lower than the stoichiometric composition (30.6 wt%). Similar deviations were found by FRANZ and SPEAR (1985) and BERNAU and FRANZ (1987).  $\text{TiO}_2$  is always lower than the ideal value of 40.75 wt%, ranging between 36.97 and 38.25 wt% with most values around 37 wt%. This is mainly due to the presence of  $\text{Al}_2\text{O}_3$ , which was detected in concentrations varying from 1.46 to 2.36 wt%. The content of  $\text{Fe}_2\text{O}_3$  remains always between 0.16 and 0.88 wt%.  $\text{MgO}$ ,  $\text{MnO}$ ,  $\text{Nb}_2\text{O}_5$ ,  $\text{Na}_2\text{O}$  and  $\text{K}_2\text{O}$  display very low values (< 0.4 wt%), whereas  $\text{V}_2\text{O}_5$  yields values up to 0.78 wt%,  $\text{Y}_2\text{O}_3$  up to 0.94 wt% and  $\text{Ce}_2\text{O}_3$  up to 1.01 wt%. No statistically significant correlations between  $\text{Al}_2\text{O}_3$ ,  $\text{Fe}_2\text{O}_3$  and  $\text{TiO}_2$  were found; the same is also true for Y, Ce and V, probably due to the EDS analytical method. Good correlations among these elements, however, are documented in the literature (e.g., CLARK, 1974; BERNAU and FRANZ, 1987). The formulae calculations yielded cation coefficients for both Si and Ca near 1.000, and hence, substitution for these elements is not important.

No essential zonation of the titanite crystals was observed; some slight chemical differences were determined but no systematic changes were seen even in backscattering electron images.

*Amphibole* is actinolitic-hornblende to magnesiohornblende in composition (Tab. 2), accord-

Tab. 2 Representative EDS-analyses of titanites, amphiboles, plagioclases and calcite from the Therapio titanite-rich carbonates.

	Titanites					Amphiboles			Plagioclases		Calcite	
	1	2	3	4	5	6	7	8	9	10	11	12
SiO <sub>2</sub>	28.43	29.05	28.79	30.70	29.86	50.86	51.38	45.11	65.55	64.20	0.28	0.40
TiO <sub>2</sub>	36.97	37.60	38.23	37.07	37.44	0.28	0.06	0.60	0.00	0.00	0.00	0.00
Al <sub>2</sub> O <sub>3</sub>	2.17	1.85	1.69	1.54	1.53	5.34	5.28	10.95	20.77	22.20	0.03	0.01
Fe <sub>2</sub> O <sub>3</sub>	0.71	0.44	0.16	0.60	0.47							
FeO						10.03	5.37	15.59	0.26	0.09	0.22	0.29
MgO	0.11	0.15	0.00	0.02	0.00	15.28	21.49	10.88	0.00	0.00	0.86	0.81
MnO	0.00	0.00	0.09	0.00	0.00	0.06	0.04	0.16	0.05	0.29	0.00	0.08
Nb <sub>2</sub> O <sub>5</sub>	0.00	0.05	0.17	0.00	0.00	0.08	0.31	0.24	0.20	0.08	0.02	0.00
CaO	28.36	28.31	28.57	27.81	27.63	12.48	12.16	11.65	2.28	2.68	50.80	50.29
Na <sub>2</sub> O	0.10	0.04	0.00	0.11	0.11	0.78	0.78	1.87	10.03	10.26	0.00	0.01
K <sub>2</sub> O	0.01	0.09	0.16	0.00	0.00	0.34	0.23	0.89	0.19	0.21	0.00	0.00
Y <sub>2</sub> O <sub>3</sub>	0.77	0.66	0.17	0.62	0.41	0.55	0.30	0.68	0.32	0.01	0.00	0.08
Ce <sub>2</sub> O <sub>3</sub>	1.53	0.88	0.41	0.67	0.69	0.02	0.04	0.11	0.00	0.00	0.00	0.19
V <sub>2</sub> O <sub>5</sub>	0.31	0.07	0.16	0.00	0.78	0.04	0.02	0.06	0.13	0.09	0.06	0.04
Total	99.47	99.19	98.60	99.14	98.92	96.14	97.46	98.79	99.78	100.11	52.27	52.20
Structural formulae on the basis of:												
	5[0]					23[0]			32[0]		6[0]	
Si	0.951	0.968	0.961	1.016	0.990	7.416	7.236	6.661	11.585	11.339	0.030	0.043
Ti	0.930	0.942	0.960	0.922	0.933	0.031	0.007	0.067	0.000	0.000	0.000	0.000
Al	0.086	0.073	0.067	0.060	0.060	0.918	0.876	1.906	4.326	4.621	0.004	0.001
Fe	0.018	0.011	0.004	0.015	0.012	1.223	0.632	1.925	0.038	0.014	0.020	0.026
Mg	0.006	0.008	0.000	0.001	0.000	3.321	4.510	2.395	0.000	0.000	0.136	0.128
Mn	0.000	0.000	0.003	0.000	0.000	0.008	0.005	0.020	0.008	0.043	0.000	0.007
Nb	0.000	0.001	0.003	0.000	0.000	0.005	0.020	0.016	0.016	0.007	0.001	0.000
Ca	1.016	1.010	1.022	0.986	0.982	1.949	1.835	1.844	0.431	0.508	5.767	5.726
Na	0.007	0.003	0.000	0.007	0.007	0.219	0.213	0.536	3.438	3.514	0.000	0.002
K	0.000	0.004	0.007	0.000	0.000	0.064	0.041	0.168	0.044	0.046	0.000	0.000
Y	0.014	0.012	0.003	0.011	0.007	0.042	0.023	0.054	0.030	0.001	0.000	0.005
Ce	0.019	0.011	0.005	0.008	0.008	0.001	0.002	0.006	0.000	0.000	0.000	0.007
V	0.007	0.002	0.004	0.000	0.017	0.004	0.002	0.006	0.016	0.011	0.004	0.003
*X <sub>Mg</sub>						0.73	0.88	0.55				
X <sub>Fe</sub>						0.27	0.12	0.45				
X <sub>an</sub>									0.11	0.13		
X <sub>ab</sub>									0.89	0.87		

Analyses 1, 2, 9 derive from Th-9e rock samples (Tab. 1), analyses 3, 10 from Th-9d, analyses 4, 5 from Th-9a, analyses 6, 7, 8, 11 from Th-10 and analysis 12 from Th-8.

\*X<sub>Mg</sub> = Mg/(Mg + Fe), X<sub>Fe</sub> = Fe/(Fe + Mg), X<sub>an</sub> = Ca/(Ca + Na), X<sub>ab</sub> = Na/(Na + Ca)

ing to the LEAKE (1978) classification. Among the trace elements Y<sub>2</sub>O<sub>3</sub> was detected in amounts up to 0.85 wt%.

**Plagioclase.** Plagioclase is acid oligoclase (Tab. 2) displaying small differences between individual crystals and inclusions in pyroxenes or amphiboles; plagioclase included in pyroxenes or amphiboles are slightly more An-rich than individuals. From the rare elements Y displays noteworthy concentrations reaching values as high as 1.10 wt% Y<sub>2</sub>O<sub>3</sub>, while Nb<sub>2</sub>O<sub>5</sub> is up to 0.29 wt%.

**Calcite** is nearly pure calcite with a very small (< 1 wt%) MgO content (Tab. 2).

**Zoisite/clinozoisite.** Zoisite/clinozoisite structural formulae were calculated on the basis of 12.5 oxygen atoms (Tab. 3). CaO ranges between 23.86 and 24.47 wt% in zoisite, and between 17.24 and 24.83 wt% in clinozoisite. Al<sub>2</sub>O<sub>3</sub> is higher in zoisite (35.05–36.19 wt%) than in clinozoisite (21.78–28.75 wt%), whereas Fe<sub>2</sub>O<sub>3</sub> is much lower in zoisite (0.65–1.92 wt%) than in clinozoisite (5.96–10.36 wt%). The pistacite content is very low in zoisite (0.01–0.03 mole%) and higher in clinozoisite (0.12–0.24). Nb<sub>2</sub>O<sub>5</sub>, V<sub>2</sub>O<sub>5</sub> and Y<sub>2</sub>O<sub>3</sub> show low values in both zoisite and clinozoisite (Nb<sub>2</sub>O<sub>5</sub>: < 0.35 wt%, V<sub>2</sub>O<sub>5</sub>: < 0.18 wt%, Y<sub>2</sub>O<sub>3</sub>:

Tab. 3 Representative EDS-analyses of zoisites, clinozoisites and pyroxenes from the Therapio titanite-rich carbonates.

	Zoisites				Clinozoisites				Pyroxenes			
	1	2	3	4	5	6	7	8	9	10	11	12
SiO <sub>2</sub>	35.90	34.38	36.66	35.71	38.70	38.30	37.61	39.72	52.61	52.82	53.52	53.79
TiO <sub>2</sub>	0.10	0.10	0.05	0.06	0.02	0.00	0.25	0.08	0.07	0.05	0.11	0.10
Al <sub>2</sub> O <sub>3</sub>	35.35	35.22	35.77	35.05	27.78	28.28	28.45	27.29	1.82	3.32	2.27	1.54
Fe <sub>2</sub> O <sub>3</sub>	1.42	1.92	0.88	1.71	6.66	6.63	6.26	6.62				
FeO									5.95	8.72	5.92	5.31
MgO	0.00	0.00	0.00	0.00	0.09	0.00	0.06	0.12	14.00	11.94	13.02	13.75
MnO	0.17	0.13	0.02	0.00	0.06	0.02	0.04	0.15	0.35	0.29	0.13	0.00
Nb <sub>2</sub> O <sub>5</sub>	0.18	0.17	0.31	0.00	0.35	0.01	0.18	0.29	0.00	0.22	0.15	0.07
CaO	24.38	24.47	23.86	24.07	23.97	24.36	23.85	23.86	23.74	21.19	22.41	23.90
Na <sub>2</sub> O	0.00	0.00	0.00	0.00	0.24	0.08	0.02	0.03	1.15	1.62	1.41	0.88
K <sub>2</sub> O	0.00	0.00	0.00	0.00	0.06	0.05	0.05	0.00	0.00	0.00	0.00	0.00
Y <sub>2</sub> O <sub>3</sub>	0.39	0.00	0.55	0.23	0.37	0.48	0.58	0.44	0.00	0.08	0.51	0.12
Ce <sub>2</sub> O <sub>3</sub>	0.04	0.35	0.00	0.00	0.00	0.00	0.04	0.00	0.04	0.00	0.26	0.17
V <sub>2</sub> O <sub>5</sub>	0.00	0.12	0.00	0.06	0.00	0.03	0.00	0.00	0.13	0.33	0.16	0.11
Total	97.93	96.86	98.10	96.89	98.30	98.24	97.39	98.60	99.86	100.58	99.87	99.74
Structural formulae on the basis of:												
	12.5[0]				12.5[0]				6[0]			
Si	2.756	2.682	2.794	2.764	3.007	2.978	2.950	3.068	1.955	1.956	1.982	1.989
Ti	0.006	0.006	0.003	0.004	0.001	0.000	0.015	0.005	0.002	0.001	0.003	0.003
Al	3.198	3.238	3.213	3.198	2.544	2.592	2.630	2.484	0.080	0.145	0.099	0.067
Fe	0.082	0.113	0.051	0.100	0.389	0.388	0.370	0.385	0.185	0.270	0.183	0.164
Mg	0.000	0.000	0.000	0.000	0.011	0.000	0.007	0.014	0.776	0.659	0.718	0.757
Mn	0.011	0.009	0.001	0.000	0.004	0.001	0.003	0.010	0.011	0.009	0.004	0.000
Nb	0.007	0.006	0.011	0.000	0.012	0.000	0.006	0.010	0.000	0.004	0.003	0.001
Ca	2.005	2.045	1.948	1.996	1.995	2.030	2.004	1.974	0.945	0.841	0.889	0.947
Na	0.000	0.000	0.000	0.000	0.035	0.013	0.003	0.004	0.083	0.117	0.101	0.063
K	0.000	0.000	0.000	0.000	0.006	0.005	0.005	0.000	0.000	0.000	0.000	0.000
Y	0.016	0.000	0.022	0.010	0.015	0.020	0.024	0.018	0.000	0.002	0.010	0.002
Ce	0.001	0.010	0.000	0.000	0.000	0.000	0.001	0.000	0.001	0.000	0.004	0.002
V	0.000	0.007	0.000	0.003	0.000	0.002	0.000	0.000	0.003	0.008	0.004	0.003
X <sub>Mg</sub>									0.81	0.71	0.80	0.82
X <sub>Fe</sub>									0.19	0.29	0.20	0.18

Analyses 1, 2 derive from Th-8 rock samples (Tab. 1), analyses 3, 4 from Th-10, analyses 5, 6 from Th-9e, analyses 7, 8, 9 from Th-9d and analyses 10, 11, 12 from Th-9a.

< 0.95 wt%), whereas Ce<sub>2</sub>O<sub>3</sub> is very low at the margins of the crystals (< 0.35 wt%), and increases considerably in the cores (2.99–4.72 wt%) resembling allanite composition.

The only well-developed relationship noticed among the elements, was the well-known negative correlation between Fe<sup>3+</sup> and Al<sup>3+</sup>.

**Pyroxene.** Clinopyroxene displays compositional inhomogeneity, occurring as patches, in the same crystal and representing diopsidic or augitic composition (Tab. 3). Notable amounts of Al (1.54–3.60 Al<sub>2</sub>O<sub>3</sub>) and Na (0.81–1.62 Na<sub>2</sub>O) are present. Small concentrations of Nb<sub>2</sub>O<sub>5</sub> (< 0.28 wt%), Ce<sub>2</sub>O<sub>3</sub> (< 0.26 wt%) and V<sub>2</sub>O<sub>5</sub> (< 0.33

wt%) were also detected. Y<sub>2</sub>O<sub>3</sub> was detected in relatively higher amounts up to 1.23 wt%.

## GEOCHEMISTRY

Representative bulk-rock compositions of some marbles and calc-silicate rocks are given in table 4. It can be seen that the MgO content of the marbles is very low, consistent with the absence of dolomite and the very low Mg content of calcite. Bulk oxidation ratios (mol%100 × 2 Fe<sub>2</sub>O<sub>3</sub>/[Fe<sub>2</sub>O<sub>3</sub> + FeO]) range from 70 to 83. The slightly higher MgO contents of the calc-silicate rocks

Tab. 4 Whole-rock analyses from representative samples of the Therapio titanite-rich carbonates.

	Th-1	Th-10	Th-9b	Th-13
SiO <sub>2</sub> wt%	6.42	56.75	56.62	6.82
Al <sub>2</sub> O <sub>3</sub>	1.33	10.45	15.77	2.58
TiO <sub>2</sub>	0.05	0.15	0.97	0.10
Fe <sub>2</sub> O <sub>3</sub>	0.70	1.77	1.85	0.83
FeO	0.00	0.72	1.30	0.72
MgO	0.83	2.00	3.30	0.83
MnO	0.02	0.05	0.06	0.02
CaO	49.00	18.90	14.70	48.90
Na <sub>2</sub> O	0.05	0.80	3.37	0.15
K <sub>2</sub> O	0.08	0.08	0.10	0.04
LOI	41.57	8.20	1.65	39.00
Total	100.05	99.87	99.69	99.99
Trace elements in ppm				
V(5)*	5	42	84	15
Y(4)	3	8	66	9
Sr(2)	277	609	848	255
Ba(5)	11	33	83	15
Zn(5)	5	26	47	12
Th(5)	0	12	86	0
Cu(10)	29	22	25	26
Ni(5)	9	63	61	13
Co(5)	2	12	16	4
Cr(5)	11	66	64	18

Numbers in brackets: detection limit.

combined with the high (relative to marbles) SiO<sub>2</sub>, Al<sub>2</sub>O<sub>3</sub>, FeO, and Na<sub>2</sub>O values are consistent with the occurrence of Al-bearing phases, Fe-Mg-silicates and titanite, found within them. Among the trace elements only Sr is present in considerable concentration.

## Discussion

### PREVIOUS STUDIES

The geological history and metamorphic evolution of the study area has not yet been worked out in sufficient detail. The broader area has been affected by three successive metamorphic episodes: 1) a high-pressure metamorphism, 2) a Barrow-type amphibolite-facies metamorphism, and 3) a greenschist-facies overprint. It is clear that the carbonate rocks and the associated gneisses and amphibolites of the "Upper Tectonic Unit" were affected by an amphibolite-facies metamorphism (LIATI and MPOSKOS, 1990).

The highest pressures assumed for the Upper Tectonic Unit of the Rhodope massif are at least 18 kbar (MPOSKOS and LIATI, 1993) corresponding to an eclogite-facies episode of Mesozoic age.

Temperatures between 630 and 700 °C and pressures between 7 and 12.5 kbar only, were determined for the least amphibolitized eclogites. These conditions do not reflect the peak of the eclogite-facies metamorphism but rather an early stage of the uplift. Pressures 7 to 9.5 kbar and temperatures of 650 to 700 °C are given for the subsequent Barrow-type amphibolite-facies overprint (LIATI and MPOSKOS, 1990).

### FORMATION OF THE IMPURE MARBLES AND CALC-SILICATE LAYERS

As it has been mentioned before, the Therapio area consists of alternating thin layers and lenses of marbles, impure marbles, calc-silicate rocks, gneisses and amphibolites. It is noteworthy that the layers or boudins of the impure marbles and/or the calc-silicate rocks are found between the marble and the gneiss or amphibolite layers.

A possible explanation for the formation of the impure marble and calc-silicate layers is:

a) They may represent local inhomogeneities in the bedding of the sedimentary protolith. This is supported by the spatial alternation of the differently composed layers.

b) Compositional changes could have been produced by a metasomatic process during the amphibolite-facies event. With metasomatism, elements and components from the amphibolites and gneisses were possibly transferred to the marble beds through circulating pore solutions or/and by diffusion of the compounds through stationary solutions.

c) Pegmatitic fluids could have been involved in the metasomatic process, as well. Additionally, these fluids could be responsible for retrogressive phenomena in the system, as the temperature dropped. The action of pegmatitic fluids could be inferred by the presence of rare elements like Y, Ce and Nb in the composition of the mineral constituents.

A combination of all the three processes could be also a possible explanation.

The local lack of re-equilibration in the mineral assemblages is, however, attributed to the last two processes.

### NATURE OF REACTIONS AND CONDITIONS OF METAMORPHISM

Because the metamorphism of the amphibolites, gneisses and carbonate rocks in the Therapio area involved mineral reactions that liberated H<sub>2</sub>O and CO<sub>2</sub>, it is likely that some intergranular



phase, rich in  $H_2O$  and  $CO_2$ , existed in the metamorphic rocks which buffered the reactions during metamorphism. Apparently, Ti, Si, Mg, Al, Fe and K were introduced during metasomatism, entering the marble layers by way of a grain-boundary phase; the presence of zoisite and titanite indicate that this fluid phase was presumably rich in  $H_2O$  relative to  $CO_2$ . The introduced elements together with the local inhomogeneities of the sedimentary protoliths produced Fe–Mg silicates, titanite and zoisite.

Within the above scenario, various reactions may have produced calcic amphibole (magnesian hornblende and actinolitic hornblende), titanite, clinopyroxene, zoisite/clinozoisite, and plagioclase in the studied carbonate rocks.

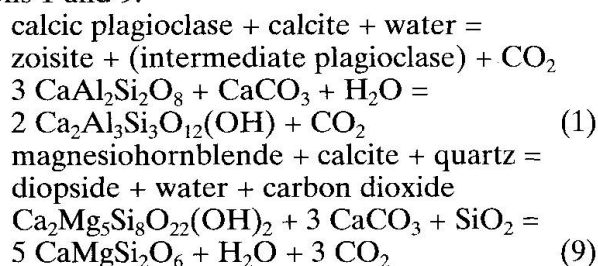
Magnesian hornblende was probably formed during the amphibolite-facies metamorphic stage (recorded in the area), from calcite, the initial impurities of the carbonate rocks and the metasomatically introduced elements. The first appearance of titanite coincides with the magnesian hornblende formation, as observed also by FERRY, (1976). Titanium mobility in hydrothermal fluids during metamorphic and metasomatic processes, can lead to the precipitation of Ti-phases (VAN BAALEN, 1993). Metasomatically formed titanite has been referred in many previous studies (e.g., SØRENSEN, 1988; GIERÉ, 1990, 1992; VAN BAALEN, 1993).

Abundant experimental information is now available on reactions and equilibria involving Ca and Mg carbonates and silicates (e.g., BERMAN 1988, 1991; McMULLIN et al., 1991). Local rock textures of the studied calc-silicate rocks were mainly used to identify the reactants forming the mineral assemblages. The mineral reactions of special interest which were used to constrain the metamorphic conditions of the studied calc-silicate rocks are:

- 1)  $3An + Cc + W = 2cZo + CO_2$
- 2)  $Sph + CO_2 = Cc + aQz + Rt$
- 3)  $Tr + 3Cc + 7CO_2 = 5Do + aQz + W$
- 4)  $Wo + CO_2 = Cc + aQz$
- 5)  $6An + Do + 2Sph + 2W = 4cZo + 2Rt + Di + 2CO_2$
- 6)  $9An + 5Di + 4W = 6cZo + Tr + 2aQz$
- 7)  $9An + 4Di + Do + 4W = 6cZo + Tr + 2CO_2$
- 8)  $33An + 5Do + Sph + 12W = 22cZo + Tr + 8Rt + 10CO_2$
- 9)  $5Di + 3CO_2 + W = Tr + 2aQz + 3Cc$
- 10)  $4Di + Do + CO_2 + W = Tr + 3Cc$
- 11)  $Tr + 8Rt + 11Cc = 5Do + 8Sph + CO_2 + W$
- 12)  $5Di + aQz + 3Rt + W = Tr + 3Sph$
- 13)  $6Rt + 11Di + 2W + 2CO_2 = Do + 6Sph + 2Tr$
- 14)  $5Di + 2Rt + CO_2 + W = Tr + 2Sph + Cc$

*Phase symbols:* An = anorthite, Cc = calcite, cZo = clinozoisite, Sph = titanite, aQz = quartz, Rt = rutile, Tr = amphibole, Do = dolomite, Di = diopside, Wo = wollastonite.

As mentioned above, diopside was observed to overgrow magnesian hornblende during the prograde stage of metamorphism, and the minerals are associated with calcite, quartz and zoisite. This assemblage can be explained by the reactions 1 and 9:



Reactions (1) and (9) are the basis of the zoisite and diopside isograds (FERRY, 1976, 1980). The conversion of plagioclase + calcite to zoisite can be explained by an introduction of  $H_2O$  into the metamorphosed carbonate rocks from amphibolites and gneisses during metamorphism. A second source of water probably was the pegmatite network; the close spatial association of zoisite-bearing meta-carbonate rocks and pegmatite veins also points to the pegmatites as a source of  $H_2O$  necessary for the reaction (1). During the following retrogressive stage, clinozoisite formed instead of zoisite as temperature dropped.

Two reasons could be considered for the oligoclase formation: One is that reaction (1) changes plagioclase composition from calcic to more sodic compositions (FERRY, 1976). The second is that metamorphism of the carbonate rocks took place under conditions of varying fluid composition (see also FERRY, 1980). In the latter case it is impossible to establish the composition of a fluid in equilibrium with the rocks when the various reactions (1) and (9) proceeded.

Clinopyroxene crystals rimmed by actinolitic hornblende clearly show that pyroxene was the reactant for this amphibole, according to the reaction (9) proceeding to the left. Such reaction is regarded as retrograde reaction. Actinolitic hornblende occurring as individual crystals means that the reaction has gone to completion. This reaction could be placed in response to an increase in the activity of  $H_2O$  relative to that of  $CO_2$ , or to a decrease in temperature. Textural features support the second alternative as more probable, and thus we accept that most reactions occurred in an environment of retrograde metamorphic conditions.

A considerable supply of  $Al_2O_3$  and  $Na_2O$  from the pegmatite veins as well as from the

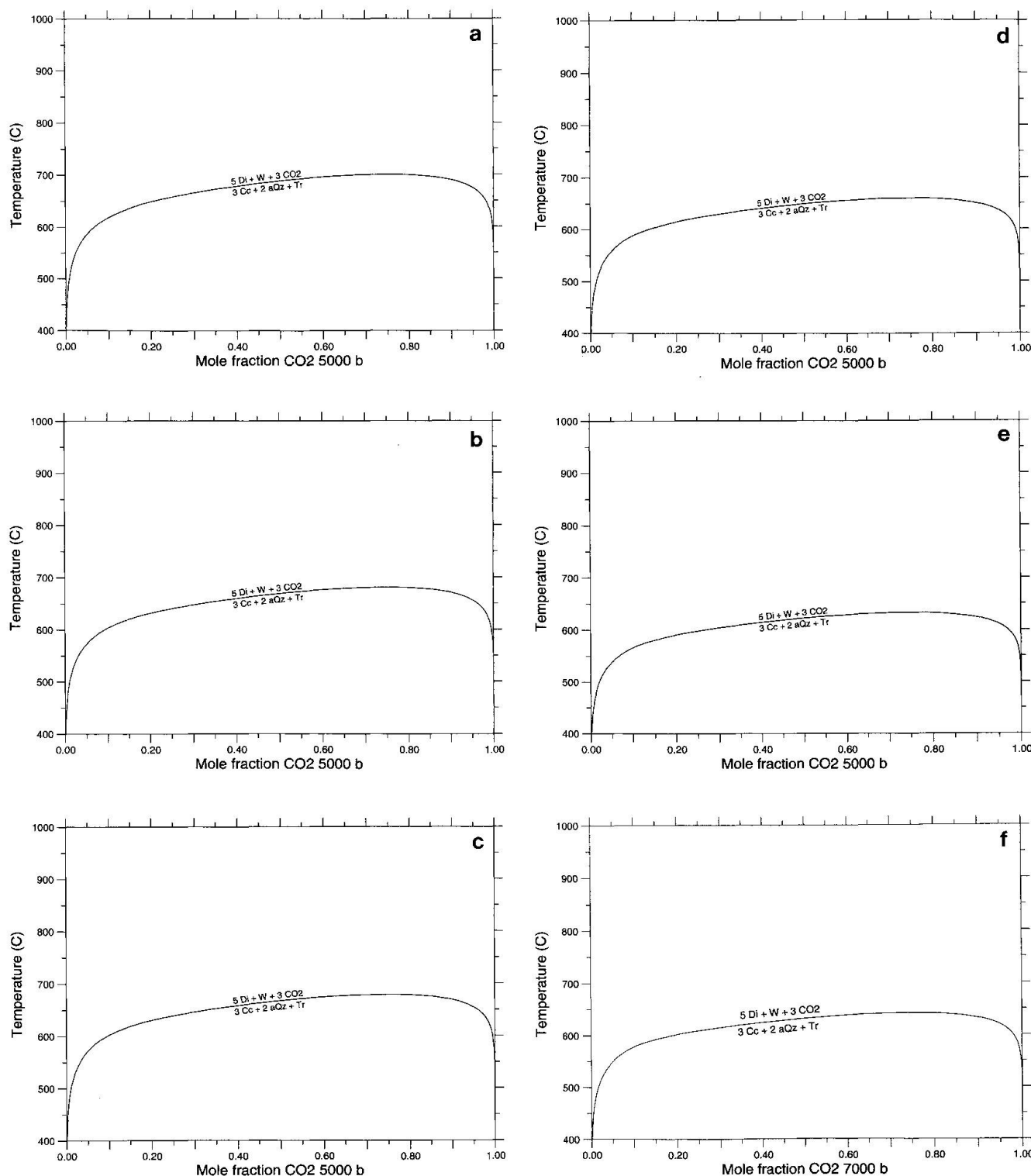


Fig. 5 Position of reaction (9) in a T- $X_{\text{CO}_2}$  diagram.

- a) assemblage: clinopyroxene + amphibole + titanite,  $a_{\text{tr}} = 0.004$ ,  $a_{\text{di}} = 0.65$   
 b) assemblage: amphibole + clinopyroxene + clinozoisite,  $a_{\text{tr}} = 0.004$ ,  $a_{\text{di}} = 0.57$   
 c) assemblage: amphibole + clinopyroxene + plagioclase + titanite,  $a_{\text{tr}} = 0.005$ ,  $a_{\text{di}} = 0.59$   
 d) assemblage: amphibole + clinopyroxene,  $a_{\text{tr}} = 0.02$ ,  $a_{\text{di}} = 0.68$   
 e) assemblage: amphibole + clinozoisite + clinopyroxene + plagioclase + titanite,  $a_{\text{tr}} = 0.06$ ,  $a_{\text{di}} = 0.69$   
 f) all activities = 1.00

Amphibole activities were calculated according to HOLLAND and POWELL (1990). For pyroxene the equation  $a_{\text{di}} = X_{\text{Ca}}(\text{M2}) \cdot X_{\text{Mg}}(\text{M1}) \cdot [X_{\text{Si}}(\text{T})]^2$  was used. Equations for H<sub>2</sub>O according to HARR et al. (1984), for CO<sub>2</sub> according to MÄDER and BERMAN (1991) and for H<sub>2</sub>O-CO<sub>2</sub> mixture according to KERRICK and JACOBS (1981).

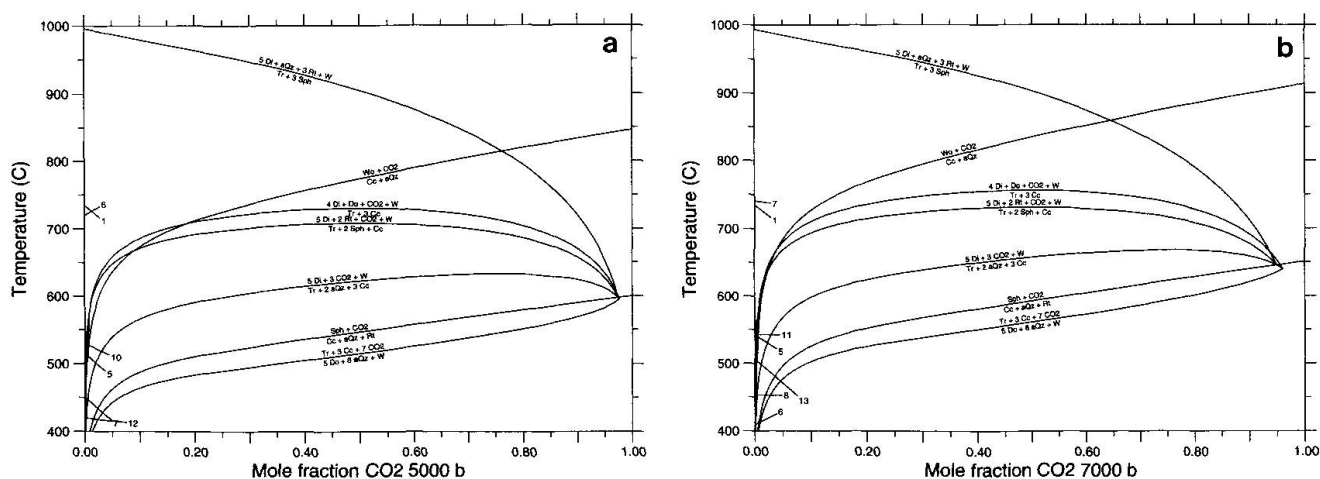


Fig. 6 T- $X_{\text{CO}_2}$  phase reaction diagrams calculated at 5 and 7 kbar. All activities calculated from assemblage e (see Fig. 5).  $a_{\text{di}} = 0.69$ ,  $a_{\text{tr}} = 0.06$ ,  $a_{\text{Cc}} = 1$ ,  $a_{\text{Oz}} = 1$ ,  $a_{\text{CO}_2} = 1$ ,  $a_{\text{H}_2\text{O}} = 1$ ,  $a_{\text{Wo}} = 1$ ,  $a_{\text{An}} = 0.1$ ,  $a_{\text{Do}} = 1$ ,  $a_{\text{Rt}} = 1$ ,  $a_{\text{Sph}} = 1$ ,  $a_{\text{cZo}} = 0.49$

gneisses gave rise to further Al-bearing minerals, e.g., biotite and muscovite.

The mineral assemblages and reaction textures preserved in these calc-silicate rocks were used to develop and evaluate petrogenetic T- $X_{\text{CO}_2}$  diagrams. Figure 5 (a, b, c, d, e) presents the position of reaction (9) curve, constructed for five assemblages at pressure 5 kbar, using calculated amphibole and clinopyroxene activities for each assemblage; figure 5f illustrates the position of the reaction (9) on the basis of pure end-members (i.e., all activities = 1.00) and at pressure 7 kbar. In the assemblages of figures 5 a, b, c and d, diopside grew at the expense of magnesiohornblende (prograde stage), while in the assemblage of figure 5e, actinolitic hornblende grew at the expense of diopside (retrograde stage). These amphibole-clinopyroxene textural relations match very well with the temperatures yielded in the phase reaction diagrams of figure 5.

Figure 6 (a, b) is an isobaric T- $X_{\text{CO}_2}$  section calculated at 5 and 7 kbar for the designated phase activities of assemblage a) (see Fig. 5). The calculations and results were checked using alternative data-sets and experimental data (KERRICK and JACOBS, 1981; BERMAN et al., 1987; MADER and BERMAN, 1991). The absence of dolomite, wollastonite and rutile and consequent absence of the reactions 2, 3, 4 and 13 from the studied parageneses, limit the area of interest below the line defined by the reaction (14) at high temperature (prograde stage) and above (2) at low temperature (retrograde stage) as can be seen in the phase reaction diagrams of figure 6. The mineral assemblage diopside + amphibole + quartz + calcite as can be inferred from figure 5 a–e, implies

a temperature range above 540 °C and below 660 °C. The pressure must not have exceeded 7 kbar.

Reaction (1) lies at the extreme left of the diagrams of figure 6, implying low  $X_{\text{CO}_2}$ .

Given the above temperatures and pressures as well as the mineral phases, the  $X_{\text{CO}_2}$  in the fluid phase is inferred to have been low, ranging between 0.1 and 0.28. The equilibrium curve calcite-anorthite-zoisite lies at low  $X_{\text{CO}_2}$  (STORRE and NITSCH, 1972; JOHANNES and ORVILLE, 1972). FERRY (1976) calculated a low (0.06–0.32)  $P_{\text{CO}_2}/(P_{\text{CO}_2} + P_{\text{H}_2\text{O}})$  value above the zoisite isograd. Moreover, the presence of zoisite/clinozoisite and titanite in the calc-silicate zones favours an extremely low  $X_{\text{CO}_2}$  (THOMPSON, 1971; HUNT and KERRICK, 1977; FERRY, 1983; HARLEY and BUICK, 1992). The considerable amount of water required to dilute the initial  $\text{CO}_2$ -rich fluids in the carbonate rocks, was possibly produced by dehydration reactions in the interlayering gneisses/amphibolites during the amphibolite facies metamorphism (see also LIATI, 1988), enhanced by the pegmatitic fluids.

## Conclusions

The impure marble and the calc-silicate layers of the Therapio area (Eastern Rhodope massif, Northern Greece) owe their unique character to local inhomogeneities of their sedimentary protoliths, which were subsequently overprinted by metasomatic processes under conditions of an amphibolite-facies metamorphism, recorded in the associated lithologies of the study area.



Additional compositional alterations of the minerals were caused by the pegmatite vein formation which crosscut all the rock types of the study area.

Phase reaction diagrams based on mineralogy and local rock textures, imply a temperature range above 540 and below 660 °C and a pressure not exceeding 7 kbar. This was the latest metamorphic overprint on the titanite-rich carbonates of the Therapio area.

The minerals formed, imply a high activity of  $H_2O$  relative to  $CO_2$ .

### Acknowledgements

We express our sincere thanks to Profs. C. de Capitani and R. Gieré for being so kind to prepare the calculations and phase reaction diagrams of this study. We also thank them for revising twice the manuscript, contributing to its very improved final version.

### References

- BERMAN, R.G. (1988): Internally-consistent thermodynamic data for stoichiometric minerals in the system  $Na_2O-K_2O-CaO-MgO-FeO-Fe_2O_3-Al_2O_3-SiO_2-TiO_2-H_2O-CO_2$ . *J. Petr.*, 29, 445–522.
- BERMAN, R.G. (1991): Thermobarometry using multi-equilibrium calculations: a new technique with petrologic applications. *Can. Mineral.*, 29, 833–855.
- BERMAN, R.G., BROWN, T.H. and PERKINS, E.H. (1987): GEOCALC: Software for calculation and display of *P-T-X* phase diagrams. *Am. Mineral.*, 72, 861–862.
- BERNAU, R. and FRANZ, G. (1987): Crystal chemistry and genesis of Nb-, V-, and Al-rich metamorphic titanite from Egypt and Greece. *Can. Mineral.*, 25, 695–705.
- BUDDINGTON, A.F., FAHEY, J. and VLISIDIS, A. (1963): Degree of oxidation of Adirondack iron oxide and iron-titanium oxide minerals in relation to petrography. *J. Petrol.*, 4, 138–169.
- CLARK, A.M. (1974): A tantalum-rich variety of sphene. *Mineral. Mag.*, 39, 605–607.
- COOMBS, D.S., NAKAMURA, Y. and VUAGNAT, M. (1976): Pumpellyite-actinolite facies schists of the Tavayanne Formation near Loèche Valais, Switzerland. *J. Petrol.*, 17, 440–471.
- DEER, W.A., HOWIE, R.A. and ZUSSMAN, J. (1982): *Orthosilicates*. Vol. 1A 2nd edition. Longman London and New York.
- DIMADIS, E. and ZACHOS, S. (1989): Geological and tectonic structure of the metamorphic basement of the Greek Rhodopes. *Geologica Rhodopica*, 1, 122–130.
- FERRY, J.M. (1976): Metamorphism of calcareous sediments in the Waterville-Vassalboro area, south-central Maine: Mineral reactions and graphical analysis. *Am. J. Sci.*, 276, 841–882.
- FERRY, J.M. (1980): A case study of the amount and distribution of heat and fluid during metamorphism. *Contr. Min. Petr.*, 71, 373–385.
- FERRY, J.M. (1983): Mineral reactions and element migration during metamorphism of calcareous sediments from the Vassalboro Formation, south-central Maine. *Am. Mineral.*, 68, 334–354.
- FRANZ, G. and SPEAR, F. (1985): Aluminous titanite (sphene) from the eclogite zone, South-Central Tauern window, Austria. *Chem. Geol.*, 50, 33–46.
- GIERÉ, R. (1990): Hydrothermal mobility of Ti, Zr, and REE: examples from the Bergell and Adamello contact aureoles (Italy). *Terra Nova*, 2, 60–67.
- GIERÉ, R. (1992): Compositional variation of metasomatic titanite from Adamello (Italy). *Schweiz. Mineral. Petrogr. Mitt.*, 72, 167–177.
- GILBERT, F., MOINE, B. and GILBERT, P. (1990): Titanites (sphenes) allumineuses formées à basse/moyenne pression dans les gneiss à silicates, Calliques de la Montagne Noire. *C.R. Acad. Sci. Paris*, 311, 657–663.
- GRAPES, R. and WATANABE, T. (1992): Paragenesis of titanite in metagreywackes of the Franz Josef-Fox Glacier area, Southern Alps, New Zealand. *Eur. J. Mineral.*, 4, 547–555.
- HARR, C., GALLAGHER, J.S. and KELL, G.S. (1984): NBS/NRC Steam Tables. Thermodynamic and transport properties and computer programs for vapor and liquid states of water in SI units. Washington: Hemisphere Publishing Co.
- HARLEY, S. and BUICK, I. (1992): Wollastonite-Scapolite assemblages as indicators of granulite pressure-temperature-fluid histories: The Rauer Group, East Antarctica. *J. Petrol.*, 33, 693–728.
- HOLLAND, T.J. and POWELL, R. (1990): An enlarged and updated internally consistent thermodynamic dataset with uncertainties and correlations: the system  $K_2O-Na_2O-CaO-MgO-MnO-FeO-Fe_2O_3-Al_2O_3-TiO_2-SiO_2-C-H_2O-O_2$ . *J. Metam. Geol.*, 8, 89–124.
- HUNT, J.A. and KERRICK, D.M. (1977): The stability of sphene: experimental redetermination and geologic implications. *Geochim. Cosmochim. Acta*, 41, 279–288.
- JOHANNES, W. and ORVILLE, P.M. (1972): Zur Stabilität der Mineralparagenesen Muscovit + Calcit + Quarz, Zoisit + Muscovit + Quarz, Anorthit + Kalifeldspat und Anorthit + Calcit. *Fortschr. Mineral.*, 50(1), 46–47.
- KERRICK, D.M. and JACOBS, C.K. (1981): A modified Redlich-Kwong equation for  $H_2O$ ,  $CO_2$ , and  $H_2O-CO_2$  mixtures at elevated pressures and temperatures. *Am. J. Sci.*, 281, 735–767.
- LEAKE, B.E. (1978): Nomenclature of amphiboles. *Can. Mineral.*, 16, 501–520.
- LIATI, A. (1988): Amphibolitized eclogites in the Rhodope crystalline Complex, near Xanthi (N. Greece). *Neues Jahrb. Mineral. Monatsh.*, H1, 1–8.
- LIATI, A. and MPOSKOS, E. (1990): Evolution of the eclogites in the Rhodope zone of northern Greece. *Lithos*, 25, 89–99.
- MÄDER, U.K. and BERMAN, R.G. (1991): An equation of state for carbon dioxide to high pressure and temperature. *Am. Mineral.*, 76, 1547–1559.
- McMULLIN, D., BERMAN, R.G. and GREENWOOD, H.J. (1991): Calibration of SGAM thermobarometer for pelitic rocks using data from phase equilibrium experiments and natural assemblages. *Can. Mineral.*, 29, 889–908.
- MAKANJOULA, A.A. and HOWIE, R.A. (1972): The mineralogy of the glaucophane schists and associated rocks from Ile de Groix, Brittany, France. *Contr. Min. Petr.*, 35, 83–118.
- MPOSKOS, E. and LIATI, A. (1993): Metamorphic evolution of metapelites in the high-pressure terrane of the Rhodope Zone, Northern Greece. *Can. Mineral.*, 31, 401–424.
- PAPANIKOLAOU, D. and PANAGOPOULOS, G. (1981): On the structural style of Southern Rhodope, Greece. *Geol. Balcanica*, 11 (3), 13–22.

- SØRENSEN, S.S. (1988): Petrology of amphibolite-facies mafic and ultramafic rocks from the Catalina Schist, southern California: metasomatism and migmatization in a subduction zone metamorphic setting. *J. Metam. Geol.*, 6, 405–435.
- STORRE, B. and NITSCH, K. (1972): Die Reaktion  $2 \text{zoisit} + 1 \text{CO}_2 = 3 \text{anorthit} + 1 \text{calcit} + \text{H}_2\text{O}$ . *Contr. Miner. Petr.*, 35, 1–10.
- THOMPSON, A.B. (1971):  $P_{\text{CO}_2}$  in low grade metamorphism: Zeolite, carbonate, clay mineral, prehnite relations in the system  $\text{CaO}-\text{Al}_2\text{O}_3-\text{SiO}_2-\text{CO}_2-\text{H}_2\text{O}$ . *Contr. Min. Petr.*, 33, 145–161.
- VAN BAALEN, M.R. (1993): Titanium mobility in metamorphic systems: a review. *Chem. Geol.*, 110, 233–249.

Manuscript received April 25, 1994; revision accepted September 3, 1995.